International Journal of Innovative Research in Advanced Engineering (IJIRAE) ISSN: 2349-2163
Issue 03, Volume 6 (March 2019) - Special Issue www.ijirae.com
SPECIAL ISSUE - 5th Inter National Level Conference - "MEEMIC – 2019"

EXTRACTION OF BLOOD CELL IMAGE CLASSIFICATION USING CONVOLUTION NEURAL NETWORK

Vignesh.U,
Guided by
V.Loganathan, Assistant Professor
Department of Medical Electronics, Sengunthar College of engineering, Tiruchengode, Tamilnadu

Manuscript History
Number: **IJIRAE/RS/Vol.06/Issue03/Special Issue/SI.MRAE10113**
Received: 20, February 2019
Final Correction: 05, March 2019
Final Accepted: 20, March 2019
Published: **March 2019**
Editor: Dr.A.Arul L.S, Chief Editor, IJIRAE, AM Publications, India
Copyright: **©2019 This is an open access article distributed under the terms of the Creative Commons Attribution License, Which Permits unrestricted use, distribution, and reproduction in any medium, provided the original author and source are credited**

Abstract-The diagnosis of blood related diseases involves the identification and characterization of a patient's blood sample. As such, automated methods for detecting and classifying the types of blood cells have important medical applications in this field. Although deep convolutional neural network (CNN) and the traditional machine learning methods have shown good results in the classification of blood cell images. Blood cells mainly include red blood cells, white blood cells and platelets. In blood, leucocyte plays an important role in the human immune function, so it is also called the immune cell. Usually, hematologists use granulated information and shape information in leukocytes to divide white blood cells into granular cells: neutrophil, eosinophil, basophil and non-granular cells: monocyte and lymphocyte. We apply the transfer learning method to transfer the weight parameters that were pre-trained on the Image Net dataset to the CNN section, and adopted a custom loss function to allow our network to train and converge faster and with more accurate weight parameters. Hence this process is applied to detect the abnormality of the cell by means of segmentation and classification. The classification results have shown an accuracy of 88.04% for KNN and 54% for ANN. The proposed system work can be further enhanced by taking other classifiers.

I.INTRODUCTION

A blood cell, also called a hematopoietic cell, hemocyte, or hematocyte, is a cell produced through hematopoiesis and found mainly in the blood. Major types of blood cells include; Red blood cells (erythrocytes).

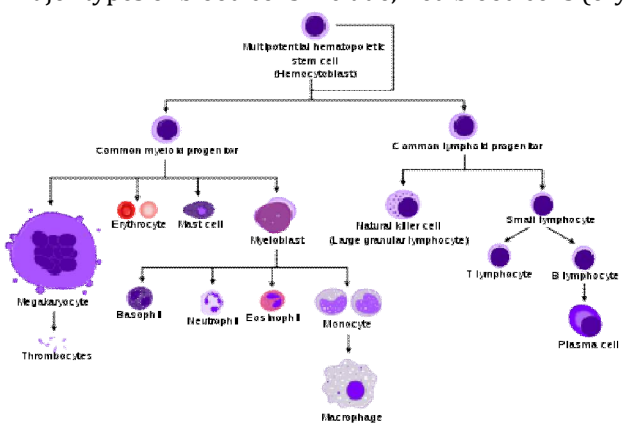

Fig.1.1 Diagram showing the development of different blood cells from hematopoietic to mature cells

IJIRAE © 2014- 19, All Rights Reserved

Together, these three kinds of blood cells add up to a total 45% of the blood tissue by volume, with the remaining 55% of the volume composed of plasma, the liquid component of blood. Red blood cells contain a protein called hemoglobin, which carries oxygen from the lungs to all parts of the body. Checking the number of red blood cells in the blood is usually part of a complete blood cell (CBC) test. It may be used to look for conditions such as anemia, dehydration, malnutrition, and leukemia. Also called erythrocyte and RBC. Finally, the computer tries to predict what's in the picture based on the prediction of all the tiles. This allows the computer to parallelize the operations and detect the object regardless of where it is located in the image.

II. PREPROCESSING

First, we need to add a little bit of variance to the

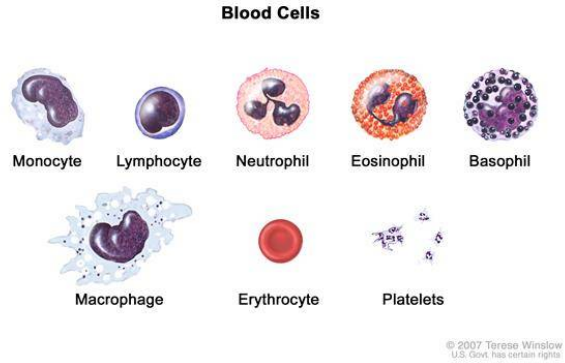

Fig.1.2 Blood cells

The average human adult has more than 5 liters (6 quarts) of blood in his or her body. Blood carries oxygen and nutrients to living cells and takes away their waste products.

II. NEURAL NETWORK

A computational model that works in a similar way to the neurons in the human brain. Each neuron takes an input, performs some operations then passes the output to the following neuron.

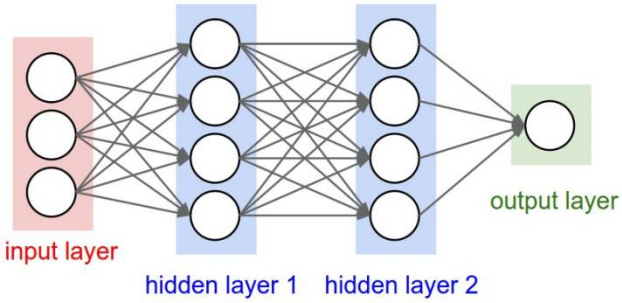

Fig.1.3 Neural Network model

One of the most popular techniques used in improving the accuracy of image classification is Convolutional Neural Networks. A special type Neural Networks that works in the same way of a regular neural network except that it has a convolution layer at the beginning. Instead of feeding the entire image as an array of numbers, the image is broken up into a number of tiles, the machine then tries to predict what each tile is. population , which makes this problem an ideal candidate for the examination of morphological heterogeneity. Unlike the normal RBCs, which are flexible and move easily even through very small blood vessels, sickle RBCs promote vaso-data since the images from the dataset are very organized and contain little to no noise. We're going to artificially add noise using a Python library named image. We're going to do a random combination of the following to the images:

- Crop parts of the image
- Flip image horizontally
- Adjust hue, contrast and saturation

Pre-processing is a common name for operations with images at the lowest level of abstraction both input and output are intensity images.

2) The RBC region and the background may have low contrast in the intensity. 3) The boundaries of RBCs may be blurry due to the influence of imaging procedure. 4) Very complex and heterogeneous shapes of RBCs are present in SCD. 5) Artifacts may be present, for instance, dirt on the imaging light path, various halos and shading. 6) Finally, because RBCs lack a nucleus, methods utilizing the nuclei location as an apparent marker for cell counting and detection are not applicable.

IJIRAE © 2014- 19, All Rights Reserved

IV.RBC WITH CONVOLUTION NEURAL NETWORK

Sickle cell disease (SCD), also known as sickle cell anemia, is a type of inherited RBC disorder associated with abnormal hemoglobin S (HbS) . When HbS molecules polymerize inside RBCs, due to lack of oxygen, they affect greatly the shape, elasticity, and adhesion properties of RBCs. Moreover, the RBCs become stiff and more fragile, with vastly heterogeneous shapes in the cell.

V. MATERIALS AND METHODS

On the basis of the raw RBC microscopy image data from SCD patients following cell density fractionation as shown in s1 appendix, our automatic, high-throughput RBC classification occlusion phenomena. Hence, SCD patients are afflicted with the risk of life-threatening complications, stroke and organ damage over time, resulting in a reduced life expectancy. According to a recent study , as of 2013 about 3.2 million people have SCD while an additional 43 million have sickle-cell trait, resulting in 176,000 deaths in 2013, up from 113,000 deaths in 1990, mostly of African origin. The prime hallmark of SCD is that is surprisingly variable in its clinical severity. Available methods for treating SCD are mainly supportive and mostly aim at symptom control, but lack the active monitoring of the health status as well as the prediction of disease development in different clinical stages.

Recent developments in advanced medical imaging technology and computerized image processing methods could provide an effective tool in monitoring the status of SCD patients. Indeed, Darrow et al. recently demonstrated a positive correlation between cell volume and protrusion number using soft X-ray tomography. Van beers et al have also shown highly specific and sensitive sickle and normal erythrocyte classification based on sickle imaging flow cytometry assay, a methodology that could be useful in assessing drug efficacy in SCD. Therefore, implementing an automated, high-throughput cell classification method could become an enabling technology to improve the future clinical diagnosis, prediction of treatment outcome, and especially therapy planning.

However, there are several major technical challenges for automatic cell classification: 1) RBCs may touch or overlap each other or appear as clusters in the image, which makes it difficult to detect the hidden edge of cells. assay consists of four main steps for the RBC-dCNN training: 1) Hierarchical RBC patch extraction, 2) Size-invariant RBC patch normalization, 3) RBC pattern classification based on deep CNN, and 4) Automated RBC shape factor calculation. A detailed overall training flowchart is shown in Fig 4. Each step of the algorithm is described below.

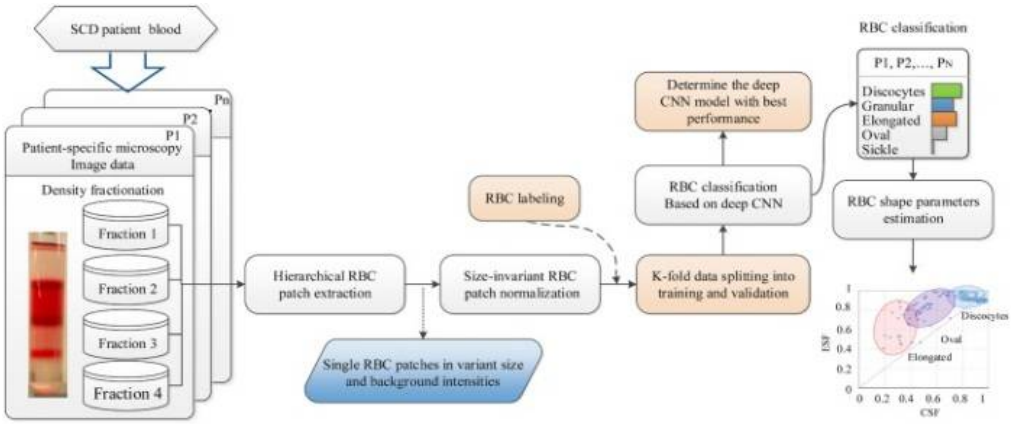

Fig.4 Overall flowchart of our proposed training and learning methodology for the sickle RBC-dCNN classification model describing the four main steps, including an independent shape factor analysis.

VI. RBC PATCH EXTRACTION

In the traditional learning-based cell image segmentation or classification method, the two most common techniques to obtain the training patches are the exhaustive pixel-wise sliding window with the same size method and the ground truth bounding box method, *e.g.* Li et al. However, the major drawback of the pixel-wise block splitting method for the application of RBC classification is that it generates a large number of unwanted and redundant patches for the background and artifacts (*e.g.*, dirt or debris in the light path) to feed for training and testing of the neural network. maximum pixel coordination (x', y') from the boundary pixels, the ROI patches are illustrated as shown in fig 6.

IJIRAE © 2014- 19, All Rights Reserved

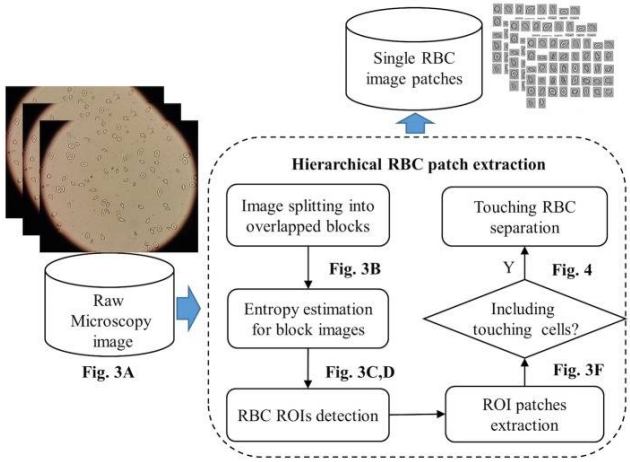

Fig.1.5Hierarchical RBC patch extraction algorithm workflow.

VII.RGB ROI REGION

we may obtain some extracted ROI regions containing multiple cells; see the yellow smaller sized box in fig 7, where 8 ROI patches contain two or more RBCs, and the pink smaller sized box that includes all segmented single RBC patches. The subimages in the two boxes were obtained by calculating the corresponding bounding boxes of the ROI. Overlapping RBCs were removed from the input of deep CNNs in our work. Therefore, we only focused on the "touching" RBC separation problem by applying the random walk method in conjunction with the distance transform to generatethe RBC boundary.

This method can obtain the.RBC seed points identification automatically. The entropy estimation method can effectively extract the complete RBC regions from the raw images, especially for those RBC boundaries in a low intensity contrast. Moreover, it can also detect the RBC region correctly from various datasets regradless of their brightness differences.Thus, it can effectively overcome the shortcomings of the previous commonly used methods (*e.g.*, Ostu, watershed and Sobel, etc.). To obtain the RBC patch images for the deep CNNs, the high-level ROI boundary is detected and by searching the minimum coordination of pixel (x_0, y_0) and

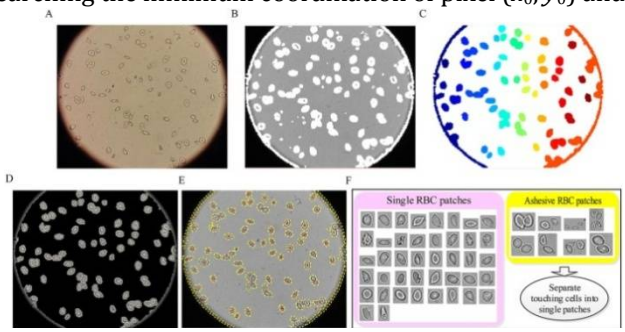

Fig.1.6 Determining ROIs and RBC patch extraction based on information from the entropy statistical estimation and morphology operations.

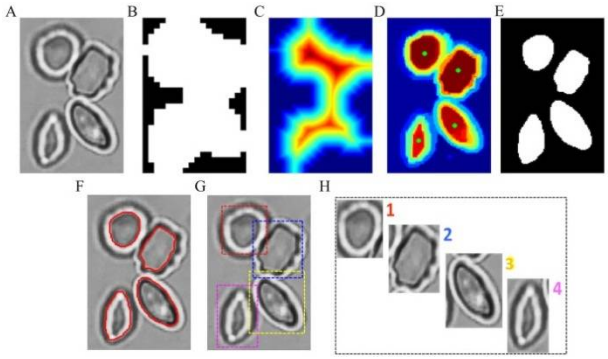

Fig.1.7 Workflow of RBC patch generation from ROIs with touching RBCs.

IJIRAE © 2014- 19, All Rights Reserved

VIII. SIZE-INVARIENT RBC PATCH NORMALIZATION

All single RBC patches in their respective various sizes were aligned at the center of their corresponding normalization mask, see in fig 8 In order to validate the performance of our method, we performed the proposed method on multiple RBC patches from different datasets with different back ground intensity distribution. Examples of the normalised size-invariant RBC patches from different datasets in Fig 8show that the RBC shape remains unaltered and staircase artifact free during the algorithmic operations.in our work, five types of data augmentation were performed on the normalized single RBC patch: rotate 90°, 180°, 270° and horizontal and vertical reflection.

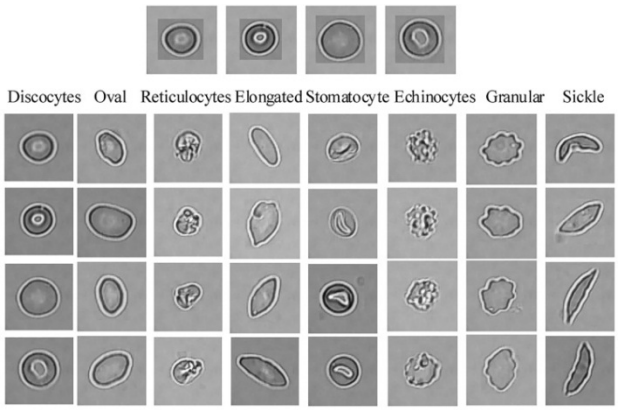

Fig1.8 Size-invariant RBC patch size normalization for eight different types of diseased RBCs

IX.RBC PATTERN CLASSIFICATION BASED ON CNN

In our work, we adopted a deep CNN architecture with 10 layers, including 3 convolutional layers ($C1$, $C3$ and $C5$), 3 pooling/subsampling layers ($P2$, $P4$ and $P6$), dropout layers ($D7$ and $D9$, where $p = 0.5$) and a fully connected layer ($F8$). As a result of the computational efficiency, the grayscale RBC image patches were initially resized to 78 * 78. Next, these were then fed into the neural network. A non-linear activation function was then applied. Following the $F7$ layer, a logistic regression method combining the softmaxfunction with a cross-entropy loss function was implemented to obtain the final learning probability and predicted labels. The softmax function can "squash" the obtained score vector $Q = \{q_i | i = 1, 2, \ldots, N\}$ to a N-dimension probability vector $\delta(q_i)$, so as to aid RBC classification efficiency.According to different shape division level for the original RBC patches, two kinds of RBC labeling principles were employed in the experiment.information derived from rotation, shifting or mirroring, illumination adjustment, etc., and introduces only a slight distortion to the images but without introducing extra labeling costs. A larger dataset can help evaluate and improve the robustness of RBC classification CNN model as well as restraining the common over-fitting problem. Thus, shape" we mention in this manuscript; moreover, wherever the state of oxygenation is not mentioned it implies "Oxy" state. We note that

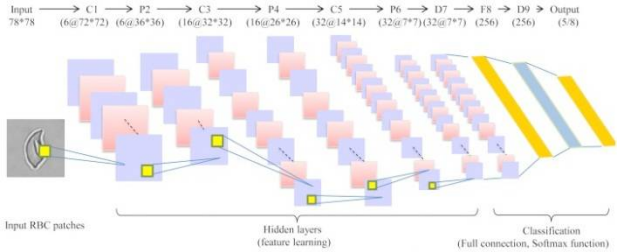

Fig1.9 Architecture of deep RBC-dCNN for SCD RBC classification.

X. CONCLUSION

In this section, we conduct several experiments to evaluate the performance of the deep CNN used in the special RBC classification cases and present a comparative analysis of the results. In our experiments in order to validate the robustness of our methodology in dealing with different imaging data, we consider 434 raw microscopy images of 8 different SCD patients collected from two different hospitals. The number of images for each patient in different fractions is shown and all the images in different fractions (F1,F2,F3,F4 and UF) are of the same size (1920*1080 pixels) in TIFF format with 4 color channels. Based on the obtained raw images, 7206 single RBC image patches were extracted by using the proposed method. Subsequently, all RBC patch images were normalized to the same size (78*78) by using the method Namely, all the RBC patch images were assigned to 8 different categories (discocytes, echinocytes, elongated, granular, oval, reticulocytes, sickle and stomatocyte) manually with the corresponding quantity of each RBC category.

IJIRAE © 2014- 19, All Rights Reserved

Conventionally, our definition of echinocytes is equivalent to echinocyte type II and III. Echinocyte type I is actually the "granular Anglin C. Sickle Cell Disease. Journal of Consumer Health on the Internet. oval shape refers to the shape of the red cells and is not related to Southeast Asian ovalocytosis. This convention is consistent in our training of the dCNN model. A comparison study on the deep CNNs training model for two datasets with different number of patients' data was conducted.

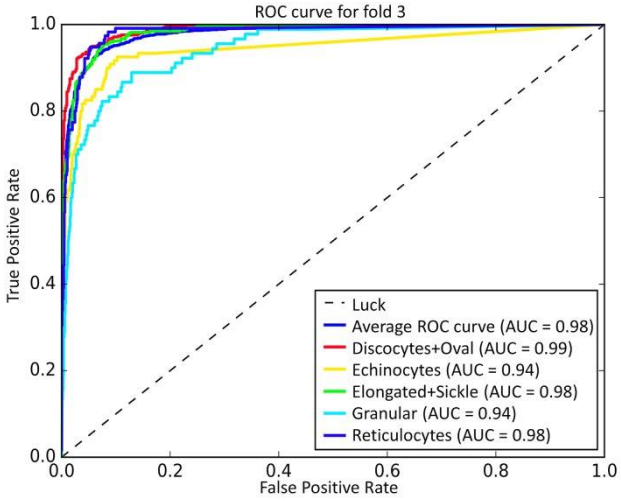

Fig1.10 ROC-AUC result for coarse 5 types of RBC classification based on "Exp_II" dataset by 5-fold cross validation.

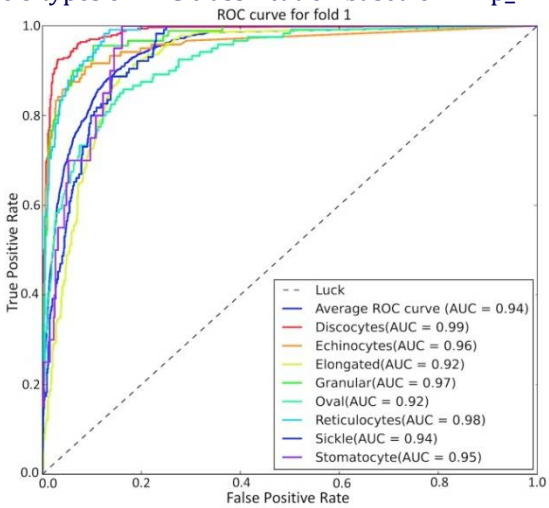

Fig1.11ROC-AUC for refined 8 types of RBC classification based on "Exp_II" dataset by 5-fold.

REFERENCES

1. He Y, Gong H, Xiong B, Xu X, Li A, Jiang T, et al. iCut: an integrative cut algorithm enables accurate segmentation of touching cells. Scientific reports. 2015;5.
2. Hodneland E, Kögel T, Frei DM, Gerdes HH, Lundervold A. CellSegm-a MATLAB toolbox for high-throughput2015;19(2):122–131.
3. Darrow MC, Zhang Y, Cinquin BP, Smith EA, Boudreau R, Rochat RH, et al. Visualizing red blood cell sickling and the effects of inhibition of sphingosine kinase 1 using soft X-ray tomography. J Cell Sci. 2016;129(18):3511–3517.
4. Donato C, Vincenzo T, Marco C, Francesco F, Maria VS, Giuseppe R. HEp-2 cell classification with heterogeneous classes-processes based on k-nearest neighbours. In: Pattern Recognition TechniquesforIndirectImmunofluorescence Images (I3A), 2014 1st Workshop on. IEEE; 2014. p. 10–15.
5. Fasano RM, Booth GS, Miles M, Du L, Koyama T, Meier ER, et al. Red blood cell alloimmunization is influenced by recipient inflammatory state at time of transfusion in patients with sickle cell disease. British journal of haematology. 2015;168(2):291–300.
6. Gao Z, Zhang J, Zhou L, Wang L. Hep-2 cell image classification with convolutional neural networks. In: Pattern Recognition Techniques for Indirect Immunofluorescence Images (I3A), 2014 1st Workshop on. IEEE; 2014. p. 24–28.

IJIRAE © 2014- 19, All Rights Reserved

7. Grady L. Random walks for image segmentation. IEEE transactions on pattern analysis and machine intelligence.
8. 3D cell segmentation. Source code for biology and medicine. 2013;8(1):16
9. Liu Z, Liu J, Xiao X, Yuan H, Li X, Chang J, et al. Segmentation of White Blood Cells through Nucleus Mark Watershed Operations and Mean Shift Clustering. sensors. 2015;15(9):22561–22586.
10. Milton JN, Gordeuk VR, Taylor JG, Gladwin MT, Steinberg MH, Sebastiani P. Prediction of fetal hemoglobin in sickle cell anemia using an ensemble of genetic risk prediction models. Circulation: Cardiovascular Genetics. 2014; p. CIRCGENETICS–113.
11. Ozpolat HT, Chang T, Chen J, Wu X, Norby C, Konkle BA, et al. Evaluation of Cell Types and Morphologies in Sickle Cell Disease with an Imaging Flow Cytometer. Blood. 2015;126(23):972–972.

IJIRAE © 2014- 19, All Rights Reserved